

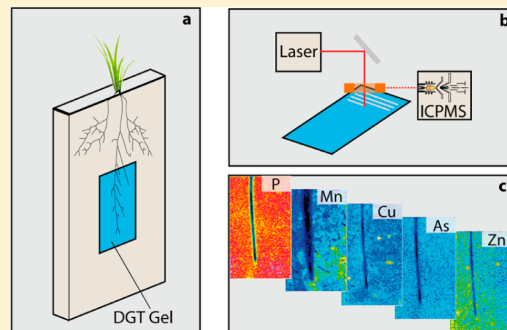
# Gel for Simultaneous Chemical Imaging of Anionic and Cationic Solutes Using Diffusive Gradients in Thin Films

Andreas Kreuzeder,<sup>†</sup> Jakob Santner,<sup>\*,†</sup> Thomas Prohaska,<sup>‡</sup> and Walter W. Wenzel<sup>†</sup>

<sup>†</sup>Department of Forest and Soil Sciences, Institute of Soil Research, <sup>‡</sup>Department of Chemistry, VIRIS Laboratory, University of Natural Resources and Life Sciences, Vienna (BOKU), Konrad-Lorenz-Strasse 24, Tulln A-3430, Austria

 Supporting Information

**ABSTRACT:** We report on a novel gel based on diffusive gradients in thin films (DGT) for the simultaneous measurement of cations and anions and its suitability for high resolution chemical imaging by using laser ablation inductively coupled plasma mass spectrometry (LA-ICPMS). The new high resolution mixed binding gel (HR-MBG) is based on zirconium-hydroxide and suspended particulate reagent-iminodiacetate (SPR-IDA) as resin materials which are embedded in an ether-based urethane polymer hydrogel. The use of this polymer hydrogel material allows the production of ultrathin, highly stable and tear-proof resin gel layers with superior handling properties compared to existing ultrathin polyacrylamide gels. The gel was characterized regarding its uptake kinetics, the anion and cation capacities, and the effects of pH, ionic strength, and aging on the performance of the HR-MBG. Our results demonstrate the capability of this novel gel for concomitant sampling of anions and cations. The suitability of this new gel type for DGT chemical imaging at submm spatial resolution in soils using LA-ICPMS is shown. 2D images of P, As, Co, Cu, Mn, and Zn distributions around roots of *Zea mays* L. demonstrate the new opportunities offered by the HR-MBG for high-resolution mapping of solute dynamics in soil and sediment hotspots, such as the rhizosphere, by simultaneous observation of anionic and cationic solute species.



It is well established that knowledge about the total concentrations of mineral elements in soil is not sufficient to infer solute mobility or availability to plants.<sup>1</sup> Therefore, a range of chemical soil extraction procedures are used to measure the bioavailable fraction of nutrients or contaminants. Some of these methods allow for the estimation of labile (readily soluble) solute fractions which are assumed to be indicators for plant availability.<sup>2,3</sup> However, chemical extractions establish a pseudoequilibrium between the soil solid phase and the extractant for a given analyte but do not mechanistically mimic solute uptake by plants. Consequently, many of these extractions only show a relatively poor correlation with plant solute uptake or plant growth response.<sup>2,4,5</sup>

Diffusive gradients in thin films (DGT) is a passive sampling technique widely used for measuring solutes in water, sediments, and soils.<sup>6–10</sup> In many cases, the DGT-labile solute fraction correlated better with the plant uptake than that measured by chemical extractants.<sup>3,10</sup> A recent isotope dilution study directly demonstrated that the DGT-labile soil P fraction is largely identical to the plant-available fraction, whereas a range of chemical extractants either under- or overestimated plant-available P.<sup>4</sup>

**DGT and Chemical Imaging.** Apart from bulk sample analysis, DGT has been applied for chemical imaging of labile solute distributions in soils and sediments since the early days of the method.<sup>11</sup> The capabilities to preconcentrate analytes in situ and to sample readily soluble solute fractions render DGT highly suitable for the investigations of nutrient and

contaminant distributions around roots. As previously suggested,<sup>10,12</sup> mechanisms of nutrient and contaminant uptake and, in some cases release, can be inferred from such chemical images.<sup>13</sup>

High-resolution chemical images of labile solutes in soils and sediments can be generated by several DGT-based approaches, i.e., (1) slicing of the gel to small pieces and measuring them individually after elution,<sup>14,15</sup> (2) computer imaging densitometry (CID),<sup>8,16,17</sup> and (3) laser ablation inductively coupled plasma mass spectrometry (LA-ICPMS).<sup>8,9,18</sup> The method of gel slicing, individual elution, and measurement of each gel piece is low-cost but tedious. Furthermore, it has high limits of detection (LOD) when compared with other methods and a spatial resolution limit of ~0.5 mm at best. CID is a simple and quick approach if a specific color reaction can be exploited. Reported spatial resolutions were in the range of 200–400 μm.<sup>8,16,17</sup> LA-ICPMS also offers high resolution (<100 μm) as well as multielement analysis at low detection limits. Previous approaches for chemical imaging using DGT gels used spot<sup>8</sup> and line ablation.<sup>13,19</sup> A comparison of both methods suggests lower LODs and lower gas consumption for line scans than for spot ablation.<sup>20</sup> The main advantage of line ablations is a high

Received: September 24, 2013

Accepted: November 20, 2013

Published: November 20, 2013



spatial resolution along the scan line and a significant reduction in measurement time.

Important properties of resin gels used for chemical imaging are a small particle size of the resin and its homogeneous distribution in the gel matrix as these may limit the resolution. Common resin materials (Chelex 100, ferrihydrite) often have a bead size >100 µm and are thus too large for imaging analysis, which has led to the development of gels with highly homogeneous distributions of low-particle-size ( $\leq 10 \text{ }\mu\text{m}$ ) sorbents. The resins used so far include suspended particulate reagent-iminodiacetate (SPR-IDA),<sup>18</sup> AgI,<sup>17</sup> and zirconium oxide,<sup>14</sup> which were added to the gel solution prior to polymerization. Some sorbents can be directly precipitated into a gel after polymerization, e.g., ferrihydrite and AgI.<sup>9,16</sup>

The suite of analytes that can be measured simultaneously is determined by the selection of resins that are incorporated into the gel. Gels for measuring cationic or anionic solutes separately at high resolution are available, but simultaneous imaging of cations and anions using one DGT gel has not been possible so far. Some recently published resin gels allow for the simultaneous measurement of anions and cations in bulk samples<sup>21,22</sup> but are not applicable for high resolution LA-ICPMS measurements because of the coarse resin materials used.

However, the concomitant imaging of anionic and cationic species is of great interest to enhance the understanding of biogeochemical processes and of element uptake by plants. For example, the phosphate distribution around roots of *Brassica napus* L. was recently investigated.<sup>13</sup> In addition to the distribution of the phosphate anion, simultaneous imaging of Fe<sup>3+</sup>, Al<sup>3+</sup>, and Ca<sup>2+</sup> is of interest, as these species could indicate the dissolution of phosphate binding sites (Fe- and Al-oxides) and mineral phosphates (Fe-, Al-, Ca-phosphates). A second example for complex, highly localized interactions of anionic and cationic species is the rhizosphere of paddy-field rice. Fe(III)-oxyhydroxides are reductively dissolved in anaerobic conditions. Due to the O<sub>2</sub> release by rice roots, Fe(II) is in turn oxidized in the vicinity of the roots and reprecipitates, forming a layer of Fe-plaque around roots. The dissolution and reformation of sorption sites for both, anions and cations, is a key factor in nutrient and contaminant dynamics in lowland rice.<sup>23,24</sup> In both environments, simultaneous DGT chemical imaging of anions and cations is of high interest. This paper presents the production, the properties, and characteristics of a novel DGT resin gel for the simultaneous high-resolution measurements of anions and cations in soils and sediments using DGT–LA-ICPMS.

## EXPERIMENTAL SECTION

**DGT Theory.** Geometrically well-defined, plastic DGT sampling devices contain a diffusive layer, commonly a polyacrylamide gel overlain by a protective membrane, and a resin gel with incorporated resin material.<sup>7,25</sup> After sampler deployment, the target analytes taken up by the resin gel are eluted and measured. This allows for the calculation of time-averaged fluxes,  $f_{\text{DGT}}$ , into the sampler and time averaged concentrations,  $c_{\text{DGT}}$ , at the sampler–solution interface:<sup>25</sup>

$$c_{\text{DGT}} = \frac{M\Delta g}{DAt} \quad (1)$$

$$f_{\text{DGT}} = \frac{M}{At} \quad (2)$$

M is the mass of analyte taken up by the resin material during the sampling time,  $\Delta g$  is the thickness of the diffusive layer (including the protective membrane), D is the diffusion coefficient of the analyte in the diffusive layer, A is the sampling window area, and t is the sampling time.

**Lab Procedures.** Wherever possible, sample handling and preparation were performed in a biological class II laminar flow bench (Clean Air, EuroFlow EF/S, Telstar Laboratory Equipment B.V., Woerden, The Netherlands). Critical sample preparation steps as well as measurements were done in a class 100,000 cleanroom. The glassware and plastics in direct contact with the gel solution or resin gels were acid washed in 10% HNO<sub>3</sub> and subsequently rinsed with laboratory water type 1 (0.055 µS cm<sup>-1</sup> provided by a TKA-GenPure purification system, Thermo Electron LED GmbH, Niederelbert, Germany) three times prior to use. All solutions were prepared using laboratory water type 1. Chemical reagents of analytical grade were used in all experiments. Sample preparation for liquid ICPMS analysis was done using laboratory water type 1 and nitric acid of reagent grade (EMSURE ISO, Merck, Darmstadt, Germany) which were further purified in-house by using a sub-boiling distillation system (Milestone Inc., Shelton, CT, USA). If not stated otherwise, DGT deployment solutions used for the characterization of the gels had an electrolyte background concentration of 10 mmol L<sup>-1</sup> NaNO<sub>3</sub> (Sigma Aldrich, Reagent Plus) and the pH was in equilibrium with ambient air (pH 5.6 ± 0.2). The deployment solutions were well stirred at 300–400 rpm using magnetic stirrers. If not stated otherwise, all measurements were done in triplicates.

All gel characterization experiments were performed for As, P, Cd, and Cu. In the pH range of our characterization experiments (3–8), these elements are predominantly present as H<sub>2</sub>PO<sub>4</sub><sup>-</sup>, HPO<sub>4</sub><sup>2-</sup>, H<sub>2</sub>AsO<sub>4</sub><sup>-</sup>, HAsO<sub>4</sub><sup>2-</sup>, Cd<sup>2+</sup>, and Cu<sup>2+</sup>. Some experiments were also performed for Co and Zn (present as Co<sup>2+</sup> and Zn<sup>2+</sup>). Because no full data set is available for the latter two analytes, this data is provided in the Supporting Information (Table S-2 and Figure S-3). Single-element stock solutions were prepared by dissolving appropriate amounts of analytical grade Na<sub>2</sub>HAsO<sub>4</sub> (Alfa Aesar, 98–102%), Cd(NO<sub>3</sub>)<sub>2</sub>·5H<sub>2</sub>O (Fluka, purum), CoSO<sub>4</sub> (Sigma, >99%), Cu(NO<sub>3</sub>)<sub>2</sub>·3H<sub>2</sub>O (Fluka, puriss), KH<sub>2</sub>PO<sub>4</sub> (Merck, pro analysi), and Zn(NO<sub>3</sub>)<sub>2</sub>·6H<sub>2</sub>O (Fluka, purum) to give a stock solution concentration of 100 mg L<sup>-1</sup>. Solutions for DGT deployment were prepared from these stocks as single element or mixed solutions depending on the experiment.

**Preparation of Diffusive and Resin Gels.** Diffusive gels with a thickness of 0.8 mm were prepared according to standard methods.<sup>7</sup> We tried to develop a Zr-hydroxide and SPR-IDA containing gel based on Ding et al.,<sup>26</sup> who describe a Zr-hydroxide-polyacrylamide resin gel for measuring phosphate. However, the addition of Zr-hydroxide to the acrylamide gel solution, both as dried and ground powder as described or as moist slurry, caused rapid acrylamide polymerization and yielded a visibly inhomogeneous Zr-hydroxide gel. Despite our efforts to improve the formulation of the gel solution, we did not succeed in obtaining homogeneous resin distribution using polyacrylamide hydrogels. It is possible that the Zr-hydroxide particles interfered with the polymerization process, as group III–VIII transition metals are known for their potential to catalyze polymerization reactions.<sup>27</sup> To overcome these problems, a urethane-based hydrogel (Hydromed D4, Advan Source biomaterials, Massachusetts, US), which has not been used for DGT gels so far, served as gel matrix for embedding

the Zr-hydroxide and SPR-IDA resins. This gel material is an ether-based hydrophilic urethane polymer which does not require UV curing or a polymerization reaction. The gel is formed upon solvent evaporation. We refer to this novel resin gel as "high resolution mixed binding gel" (HR-MBG) throughout this paper.

A total of 15 g of  $\text{ZrOCl}_2 \cdot x\text{H}_2\text{O}$  (Alfa Aesar, 99.9985%) was dissolved in 500 mL of laboratory water type 1. Zirconium hydroxide precipitate was prepared by titrating this solution with a 0.1 mol L<sup>-1</sup> NaOH (Alfa Aesar, 99.99% metals basis) solution under vigorous stirring until the pH stabilized at 7.0. The solution containing the precipitated Zr-hydroxide was filtered using a vacuum flask and a Buchner-funnel (VWR 454, quantitative filter paper). Subsequently, the precipitated Zr-hydroxide was washed by adding 5 L of laboratory water type 1 to the funnel and sucking the water off until only the slurry remained on the filter. The moist precipitate was transferred into acid-washed containers and stored at 6 °C. A batch of 15 g of  $\text{ZrOCl}_2 \cdot x\text{H}_2\text{O}$  yields approximately 140 g of precipitate (wet weight).

Ten grams of the hydrogel material Hydromed D4 was crushed to ~5 mm pieces and dissolved in 100 mL of an ethanol (Sigma, Aldrich, puriss)-laboratory water type 1 solution (10:1, v/v). Fifteen grams of the Zr-hydroxide slurry was transferred into an acid washed polypropylene container. Approximately 90 mL of Hydromed solution was added to yield 100 mL of the Zr-hydroxide–Hydromed mixture. This mixture was homogenized with a dispersing device (Ultra-Turrax T10 Basic, IKA-Werke GmbH & CO. KG, Staufen, Germany) at ~20,000 rpm for 5 min. One milliliter of suspended particulate reagent iminodiacetic acid (SPR-IDA; CETAC Technologies, Nebraska, US) resin was added to 9 mL of Zr-hydroxide–Hydromed solution and vigorously shaken by hand for 3 min. This solution was then fixed in an overhead-shaker and rotated at 2–3 rpm overnight to eliminate air bubbles from the viscous gel solution.

An acid-washed plastic spacer with a thickness of 0.25 mm was arranged on a glass plate in a U-shape (approximately 6 × 20 cm in size) and fixed on the outer side with small strips of adhesive tape. A layer of hydrogel was coated onto a glass plate by consecutively applying three thin layers of gel on top of each other. Therefore, approximately 3 mL of bubble-free gel solution was poured into the spacer and evenly distributed within using a second glass plate as a coating tool. The glass plate with the freshly coated gel solution was put into an oven at 80 °C until the gel was dry (approximately 10 min). Afterward, the hot glass plate was allowed to cool to room temperature in a clean bench, and the coating process was repeated two more times to achieve a triple coating. The triple-coated gel was allowed to cool to room temperature. The spacer was removed, and the outer 2 mm of the gel sheet was cut off using a razor blade to remove areas with inhomogeneous resin distribution along the gel edges. The gel sheet with the glass plate was put into 5 L laboratory water type 1 for at least 4 h to hydrate. Afterward, it was gently detached from the glass plate using tweezers and placed in a fresh water bath of 5 L laboratory water type 1 for full hydration for 24 h.

With this procedure, a 100 μm-thick gel with highly homogeneous resin distribution was produced. The thin gel is a result of solvent removal during the drying process where the solvents, especially ethanol, are evaporated at 80 °C. A circular metal die-cutter had to be used to cut gel discs, as the gel is very stable and tear-proof. Teflon-coated razor blades

were used for cutting rectangular gel pieces. The hydrated gel was stored in 10 mmol L<sup>-1</sup> NaNO<sub>3</sub> solution at 6 °C.

DGT devices as provided by DGT Research Ltd. (Lancaster, UK) were used for the solution experiments. These samplers are designed to host a sampling setup consisting of 0.4 mm of resin gel, 0.8 mm of diffusive gel, and 0.14 mm of protective membrane. To compensate for the HR-MBG gels being thinner than common resin gels, a 0.4 mm plastic spacer was placed at the bottom of the sampler. This assembly was used throughout the solution experiments. If only the gel discs were deployed without the sampling device, this is noted in the experimental description.

**Digestion of Gel Discs and Matrix Evaporation.** In preliminary tests, we found poor reproducibility and low elution efficiencies for elution of analytes from the HR-MBG in both, acidic and alkaline, solutions. Therefore, the resin gels were subjected to microwave-assisted digestion in 5 mL of HNO<sub>3</sub> and 1 mL of H<sub>2</sub>O<sub>2</sub> (Fluka, TraceSELECT) using a Multiwave 3000 (Anton Paar, Graz, Austria) microwave instrument for measuring the amount of analyte taken up by the gels. In this way, complete recovery of the analytes was achieved (see Results and Discussion). Moreover, a source of uncertainty for calculating  $c_{\text{DGT}}$ , i.e., the analyte recovery factor, was eliminated.

The digests were diluted to achieve a HNO<sub>3</sub> concentration of ~2% (m/m). In case this dilution step was expected to result in analyte concentrations lower than 1 μg L<sup>-1</sup>, matrix evaporation of the digests was performed for preconcentrating the analytes prior to analysis. The evaporation was done at 90 °C for 15 h in perfluoroalkoxy-vials. Preconcentration factors of ~18 were achieved in this way.

**Analysis of Samples.** The determination of the elemental concentration of liquid samples was performed on a Thermo Fisher ELEMENT XR (Thermo Fisher Scientific, Bremen, Germany) ICPMS. As internal normalization standard <sup>115</sup>In was found to be unsuitable, because of Zr-based interferences arising due to the high Zr concentrations in gel digests. Therefore, <sup>72</sup>Ge and <sup>89</sup>Y were used as internal standards for all measurements. The certified reference material SpS-SW2 (Surface Water Level 2, Batch 126, Spectrapure Standards, Oslo, Norway) was measured together with a custom assurance standard (SPEX CertiPrep, NJ, US) for validation.

**Laser Ablation ICPMS.** Chemical imaging was accomplished by LA-ICPMS with a UP 193-FX (ESI, NWR Division, CA, US) laser ablation system coupled to a NexION 300 ICPMS (Perkin-Elmer, MA, US). The quadrupole ICPMS was chosen for the imaging experiment because of shorter measurement cycles while providing enough sensitivity for the investigated analytes.

The laser spot size was set to 100 μm, the line scanning speed to 100 μm s<sup>-1</sup>, the laser pulse frequency to 15 Hz, and laser energy output to 15%, which equals 11–12 J cm<sup>-2</sup>. Helium was used as sample gas at a flow rate of 0.9 L min<sup>-1</sup>. This gas stream was mixed with the nebulizer gas stream (Ar 1 L min<sup>-1</sup>) prior to introduction into the ICPMS.

The used settings were optimized for an ablation area of 2.1 × 3.5 cm, which was analyzed in a 4 h measurement run yielding ~23,000 readings (including the washout periods after each line). The dwell times of all analytes were adjusted to provide sufficient sensitivity.

The background equivalent concentrations (BEC) for all analytes used in the chemical imaging experiment were determined. As internal standard, <sup>13</sup>C was chosen as has been

done earlier for different DGT gels.<sup>20,28</sup> All signals were corrected for the gas blank. Data processing was done in MS Excel, and visualization was performed using the ImageJ software (National Institute of Health, Maryland, US), which is free to download at <http://rsbweb.nih.gov/ij>.

**Preparation of Calibration Standards for LA-ICPMS.** Standards for LA-ICPMS were prepared by deploying HR-MBG gels in DGT samplers in 3 L of deployment solution at varying analyte concentrations and deployment times. Each treatment was replicated 4 times.

After retrieval, one of the gels was put on a polycarbonate membrane (Nuclepore Track-Etched Membrane 0.2  $\mu\text{m}$ , Whatman, UK) and dried in a gel drier (Unigeldryer 3545, Labgeräte und Vertriebs GmbH, Martinsried, Germany). The gel stuck inseparably to the membrane after drying. This gluing effect prevented the gel from shrinking during the drying process. The membrane with the dried HR-MBG was subsequently mounted on a glass plate for laser ablation analysis.

The analyte loading of the gel discs was determined by digestion of the three remaining gels and measurements of the solutions by liquid ICPMS. The corresponding LA-signal intensity was determined by measuring 4 lines on the remaining fourth gel with LA-ICPMS. Two horizontal and two vertical lines were ablated over the gel disc. This method of determining the gel loading and corresponding signal intensity is a full matrix match of gel standards for laser ablation and gel samples.

## ■ CHARACTERIZATION OF DGT PERFORMANCE

**Gel Hydration.** The hydration characteristics of the resin gel were investigated by measuring the size of a gel strip with a ruler after the removal of the gel sheets from the glass plate but prior to any contact with water. The strips were placed subsequently into laboratory water type 1, and the increase in length during gel hydration after predetermined time intervals was measured.

**Kinetics of Uptake and Recovery of Analytes.** Kinetics of uptake were investigated by deploying HR-MBG discs in analyte solutions and measuring the uptake of analytes. To investigate the recovery of analytes, a mass balance was computed. The gel discs were placed in vials containing 10 mL of uptake solution and were shaken on a horizontal shaker during deployment. The uptake solution contained  $580 \pm 15 \mu\text{g L}^{-1}$  As,  $590 \pm 24 \mu\text{g L}^{-1}$  P,  $460 \pm 9.0 \mu\text{g L}^{-1}$  Cd,  $610 \pm 15 \mu\text{g L}^{-1}$  Co,  $540 \pm 12 \mu\text{g L}^{-1}$  Cu, and  $520 \pm 4.6 \mu\text{g L}^{-1}$  Zn at the beginning of the experiment. The gels were exposed to the solution for time intervals of 1, 3, 6, 10, 30, 60, 120, 300, and 1440 min. The initial analyte concentration in solution and the concentration of the solution after exposure to the discs were measured to calculate the mass balance. The gel discs were digested, and the digests were measured for their analyte concentrations. The analyte recovery of the digestion procedure was determined.

**Capacity.** The capacity of the HR-MBG was determined for Cd and P by deploying DGT samplers for 5 h in 3 L solutions containing both P and Cd, at concentrations of 0.52, 1.32, 2.63, 7.37, 13.5, 19.4, 27.5, 36.8, and 46.1  $\text{mg L}^{-1}$  P and 0.52, 1.29, 2.46, 7.13, 20.3, 37.0, 64.0, and 112.7  $\text{mg L}^{-1}$  Cd. Cd was chosen for determining the cation capacity, as the iminodiacetic acid group has a relatively low selectivity toward Cd; therefore, the determined capacity values are applicable to cations with higher selectivity (Cu, Ni, Pb, Zn, Co).<sup>29</sup> To investigate Cd–P

interactions that were observed at very high ion concentrations, deployments in single-element solutions were also performed. Therefore, solutions of 4.93, 14.2, 14.9, 23.4, and 38.9  $\text{mg L}^{-1}$  P and solutions containing 15.7, 25.3, 49.9, 91.1, and 120  $\text{mg L}^{-1}$  Cd were prepared separately.

**pH, Ionic Strength, and Aging.** Possible effects of solution pH, ionic strength, and increasing gel age on the uptake of analytes were tested by deploying DGT samplers for 5 h in 3 L analyte-containing solutions (As, P, Cd, and Cu) with varying pH and ionic strength.

The pH of laboratory water type 1 with 10  $\text{mmol L}^{-1}$   $\text{NaNO}_3$  background concentration was adjusted to 3, 4, 5, 6, 7, and 8 by adding 0.1 mol  $\text{L}^{-1}$  NaOH or  $\text{HNO}_3$  and letting the solution equilibrate several times (depending on the pH change but at least two times) in the course of two days under ambient conditions. When the pH had stabilized, the stock solutions containing the analytes were added. Separate solutions for the anionic and cationic species were prepared to prevent precipitation for the experiments at pH 7 and 8. The pH was monitored throughout the experiment.

The ionic strength was adjusted to 0.001, 0.01, 0.1, and 0.5 mol  $\text{L}^{-1}$  by adding  $\text{NaNO}_3$ . All solutions had a pH of  $5.6 \pm 0.2$ . The performance of the gels with increasing age was investigated by deploying HR-MBG gels of one production batch in DGT samplers into analyte solutions 14, 28, 47, and 91 days after production. In all experiments, subsamples of the deployment solution were taken at the beginning and the end of the experiment and measured for their analyte concentrations.

**Limit of Detection and Limit of Quantification.** The limit of detection (LOD) and limit of quantification (LOQ) were determined by analyzing six blank HR-MBG discs after digestion. The measurement for the analyte content used exactly the same sample preparation procedure as for all other samples. The LOD was calculated by multiplying the standard deviation of the blanks by a factor of 3 and the LOQ by a factor of  $10^{30}$ .

**Chemical Imaging of DGT-Labile Anionic and Cationic Solute Species in Soil.** A plant experiment was conducted to demonstrate the suitability of the HR-MBG for the simultaneous chemical imaging of anions and cations in soil. The procedure followed the work of Santner et al.;<sup>9</sup> an overview is given in Figure S-1, Supporting Information. A flat growth box (termed rhizotron) with a removable front window was filled with a Cambisol topsoil<sup>31</sup> from a fertilized agricultural plot (“Spöcklberg”, Lamprechtshausen, Austria). The soil surface was covered by a layer of a 10  $\mu\text{m}$ -thick polycarbonate membrane (Nuclepore, Whatman, UK) to protect the plant roots when opening the rhizotron for gel application.

For solute sampling, the soil was moistened to 30% maximum water holding capacity by adding water through irrigation holes located at the back side of the rhizotron. A *Zea mays* L. seedling was transplanted to the rhizotron just after the first root tip had emerged from the seed. After 5 days of growth, the rhizotron was carefully opened and the soil was water-saturated by adding water through hoses attached to the irrigation holes. An approximately  $3 \times 5 \text{ cm}$  large piece of HR-MBG was placed onto the membrane-covered soil surface across a living root. In addition to protecting the root, the polycarbonate membrane also served as a 10  $\mu\text{m}$  thick diffusion layer. For reducing image blurring by lateral diffusion of P in the diffusion layer, no additional diffusive gel was used. Afterward, the rhizotron was closed by putting the cover

plate back in place. Thereby, gentle pressure was applied to the HR-MBG, ensuring close contact of the soil, the Nuclepore membrane, and the resin gel. As thin films of the HR-MBG are semitransparent, the entrapment of air bubbles between soil, membrane, and gel could be excluded by visual inspection. Analyte uptake was allowed for 24 h. Afterward, the HR-MBG was retrieved from the rhizotron and dried as mentioned earlier.

## RESULTS AND DISCUSSION

**Gel Properties.** The newly developed procedure of coating ether-based urethane polymer resin gels containing SPR-IDA and zirconium-hydroxide results in ultrathin ( $\sim 100 \mu\text{m}$ ) and highly stable gels. Ultrathin gels allow for the application of a second layer of a planar sensor at the back of the resin gel, for example, a second DGT gel or a planar optode.<sup>32</sup> In a dual-layer setup, a thin first sampling layer is vital for minimizing image blurring in the underlying second layer by diffusive relaxation during analyte passage through the first layer. Compared with the acrylamide-based  $\sim 100 \mu\text{m}$  thick DGT gel described by Lehto et al.,<sup>28</sup> our ether-based urethane polymer gel is much more stable and tear-proof and requires no supporting membranes during gel handling.

**Gel Hydration.** Hydrogels swell once placed in water.<sup>33</sup> The hydration characteristics of the HR-MBG are shown in Figure S-2, Supporting Information. The maximum expansion was reached after 24 h at 135% (STD = 0.2%,  $n = 3$ ) of the initial gel size. Similar to common diffusive gels based on acrylamide, the resin gel was fully hydrated within one day and did not show any change in size during a further one-week period. Thus, we recommend gel hydration for 24 h in 5 L of laboratory water type 1 and changing the water once.

**Kinetics of Uptake and Analyte Recovery.** The mass of analytes bound onto the HR-MBG increased linearly for the first 60 min after which the binding rate decreased as the solution approached total depletion (Figure 1). Maximum uptake was reached after 300 min when the deployment solutions were effectively free of analytes. The analyte uptake rates of the HR-MBG were similar to values reported by Mason et al.<sup>22</sup> Therefore, it is concluded that there is no kinetic limitation of uptake. The HR-MBG thus acts as an infinite sink which is a prerequisite for its use in DGT deployments.

The digestion followed by sample dilution and, if necessary, matrix evaporation, showed analyte recoveries of  $103 \pm 5\%$  for As,  $95 \pm 11\%$  for P,  $107 \pm 6\%$  for Cd, and  $100 \pm 8\%$  for Cu (STD,  $n = 21$ ). These values are very close to 100% recovery, and their standard deviations are in the range of values reported for other resin gels with complete analyte recovery by acid elution.<sup>6,9,34</sup> To our knowledge, a full acid digestion of resin gels using microwave-assisted digestion has not been used so far. Complete recovery was achieved with open digestion systems on two occasions.<sup>34,35</sup> We adopt 100% recovery for the applied digestion procedure as the standard deviations in the recoveries overlap the 100% margin for all but Cd where the recovery was slightly higher.

**Capacity.** A region of linear DGT uptake of P and Cd was observed for single element solutions as well as for the solutions containing both species (Figure 2). The uptake of P onto the HR-MBG followed the theoretically predicted values up to  $\sim 7 \mu\text{g cm}^{-2}$  ( $0.23 \mu\text{mol cm}^{-2}$ ) P and  $\sim 35 \mu\text{g cm}^{-2}$  ( $0.31 \mu\text{mol cm}^{-2}$ ) Cd, calculated as accumulated mass divided by the total gel disc area (here  $4.52 \text{ cm}^2$ ). These values were adopted as maximum gel capacities. For comparability, the reported

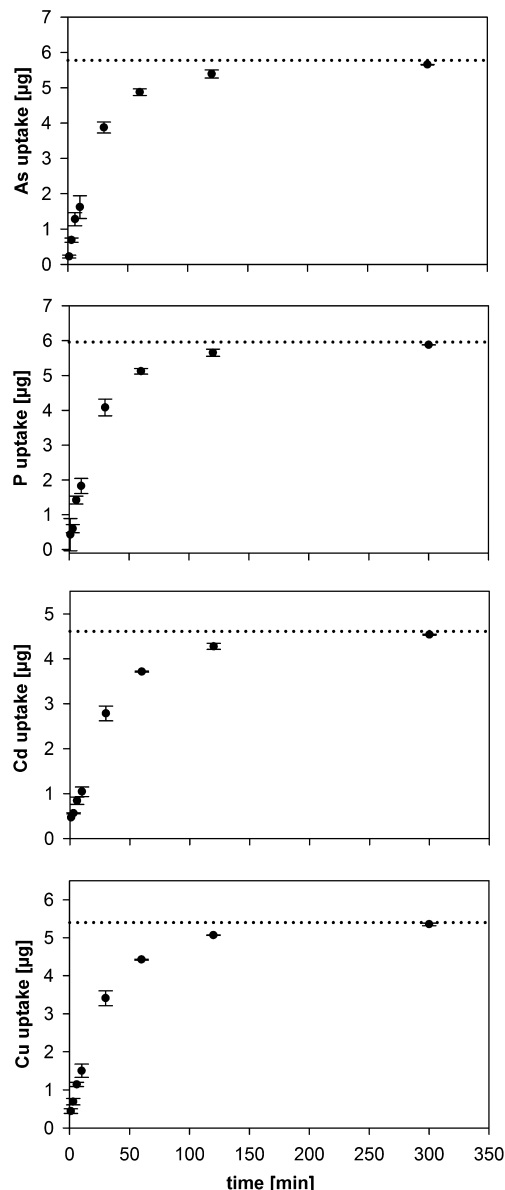


**Figure 1.** Uptake of As, P, Cd, and Cu onto gel discs from multielement solutions containing  $4.6 \mu\text{g}$  of Cd,  $5.4 \mu\text{g}$  of Cu,  $5.8 \mu\text{g}$  of As, and  $5.9 \mu\text{g}$  of P in 10 mL after immersion for 1, 3, 6, 10, 30, 60, 120, and 300 min (1440 min not shown here). The dotted line shows the content of analyte in  $\mu\text{g}$  in the 10 mL of uptake solution. Error bars represent the standard deviation of the mean ( $n = 3$ ).

literature values were recalculated to values based on the total gel disk area. In single element solutions containing either Cd or P, further uptake above this threshold was lower than theoretically expected on the basis of the calculation of mass uptake according to eq 1. However, in multielement solutions containing Cd and P, Cd uptake according to eq 1 beyond the determined capacity was observed. For P, no such increased uptake was seen; however, at high Cd and P concentrations ( $>35 \text{ mg L}^{-1}$  P,  $>35 \text{ mg L}^{-1}$  Cd), a sharp decrease of P uptake was observed. The increased Cd uptake in the presence of phosphate could be caused by changes in the surface charge of the Zr-hydroxide surface. Phosphate ions binding to the Zr-hydroxide will render the average surface charge more negative, which could lead to Cd binding to the hydroxide. The decrease in phosphate uptake seems to be an interactive effect that is

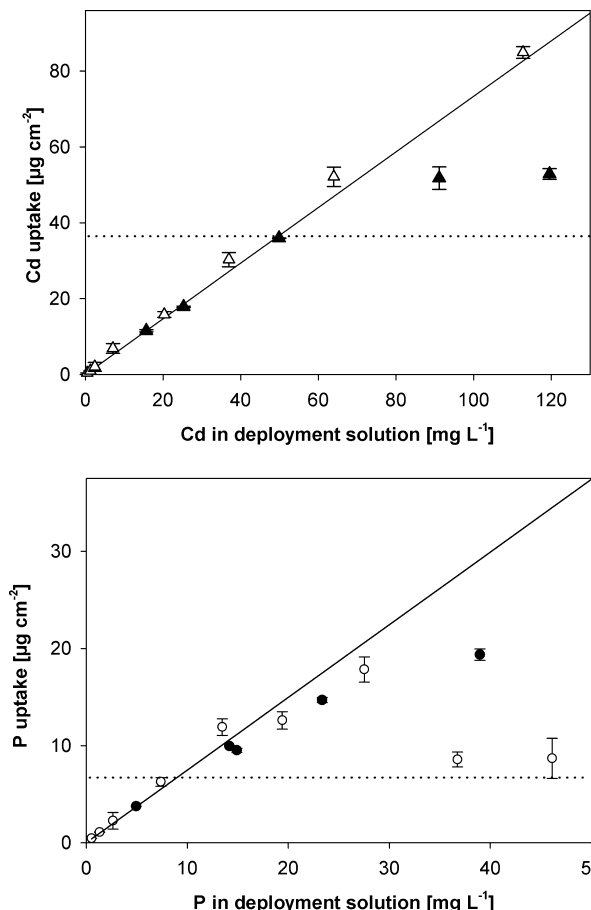


**Figure 2.** Capacity of the gel for P and Cd. Measurement after 5 h of deployment in P- and Cd-containing solutions at various concentrations (open symbols) and single element solutions (filled symbols). The solid line shows the theoretically accumulated mass in DGT samplers according to eq 1. Error bars represent the standard deviation of the mean ( $n = 3$ ). The dotted lines represent the maximum capacity defined for the HR-MBG.

caused by the high external Cd concentrations. Similar interactions were recently reported for a Chelex 100–ferrihydrite resin gel, where the As uptake decreased in the presence of metal cations (Cd, Cu, Zn, Pb).<sup>36</sup> However, we did not study these interactions further as they only occurred at very high external Cd and P concentrations, which are unlikely to occur even in highly contaminated or overfertilized environments. In uncontaminated, natural soils, solute concentrations of the analytes targeted by this resin gel are often in the range of 0.1–500  $\mu\text{g L}^{-1}$ .<sup>37</sup> In such environments, interactive effects as seen in this experiment should not occur. Measurements in highly contaminated environments at high solute concentrations, however, require thorough evaluation.

Given the lower affinity of the iminodiacetic acid group<sup>29</sup> for  $\text{Cd}^{2+}$  compared to  $\text{Co}^{2+}$ ,  $\text{Cu}^{2+}$ , and  $\text{Zn}^{2+}$ , the Cd capacity determined here is also the capacity threshold for these other ion species. Furthermore, as the phosphate concentration in uncontaminated environments is usually much higher than the arsenate concentration and the affinity of Zirconium hydroxide/oxide for both ion species is similar, the determined capacity for P is also the capacity threshold for As.<sup>38</sup>

The P capacity of the HR-MBG with 7  $\mu\text{g cm}^{-2}$  is similar to that of a gel containing precipitated ferrihydrite (6.94  $\mu\text{g cm}^{-2}$ )<sup>9</sup> higher than conventional ferrihydrite gels (1.36  $\mu\text{g}$

$\text{cm}^{-2}$ )<sup>6</sup> and a mixed binding layer also based on ferrihydrite (2.45  $\mu\text{g cm}^{-2}$ )<sup>22</sup> but lower than a high-capacity gel based on Zr-hydroxide/oxide (~100  $\mu\text{g cm}^{-2}$ ).<sup>26</sup> The Cd capacity with 35  $\mu\text{g cm}^{-2}$  (0.31  $\mu\text{mol cm}^{-2}$ ) is significantly lower than for standard Chelex 100 gels (~115  $\mu\text{g cm}^{-2}$ ).<sup>7</sup> Compared with another mixed binding gel described by Mason et al. (15.3  $\mu\text{g Mn cm}^{-2} \triangleq 0.28 \mu\text{mol cm}^{-2}$ ) the capacity seems slightly higher, however, not considering that the affinity of Chelex for Mn is lower than for Cd.<sup>22</sup> Despite the lower cation capacity compared to standard Chelex gels, our gel has sufficient capacities of As, Cd, P, and Cu for deployment in uncontaminated environments.

**pH, Ionic Strength, and Aging.** DGT-measured element concentrations agreed well with the directly measured deployment solution concentrations in a range of pH 4–8 (Figure 3).

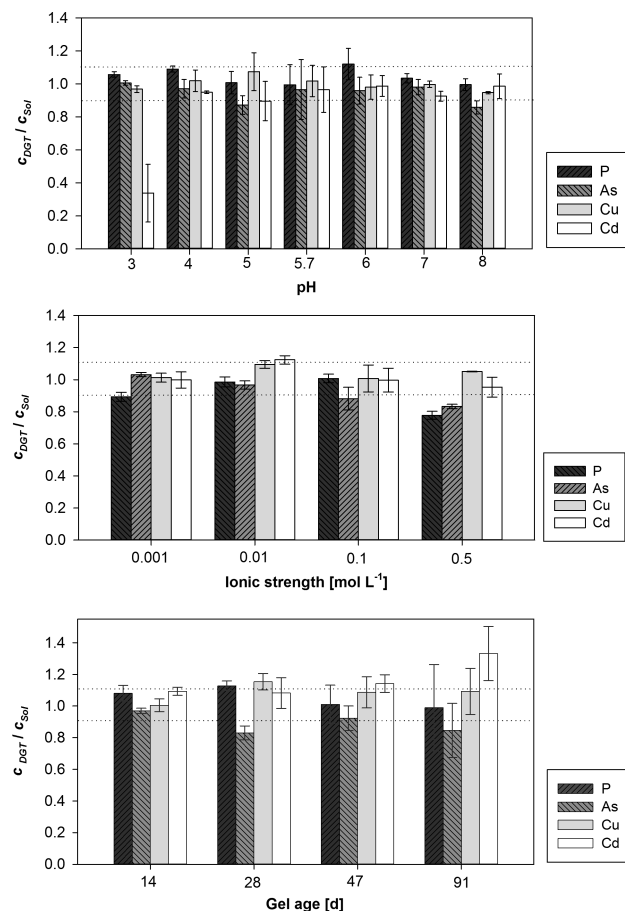


**Figure 3.** Gel performance shown as the ratio of  $c_{\text{DGT}}$  to the deployment solution concentration ( $c_{\text{Sol}}$ ) affected by (a) pH, (b) ionic strength, and (c) age of the gel. The dotted lines denote the range of  $1 \pm 0.1$ . Error bars represent the standard deviation of the mean ( $n = 3$ ).

At pH 3, Cd uptake was strongly reduced, which is in line with the known pH dependency of Cd sorption by iminodiacetic acid. The uptake of P, As, and Cu at pH 3 was close to 100%. Due to its high affinity to the iminodiacetic acid group,<sup>29</sup> Cu was still taken up quantitatively at this low pH.

The performance of the HR-MBG was affected only at high ionic strengths. In the ionic strength range of 0.001 to 0.1  $\text{mol L}^{-1}$ , the uptake was within expectations (Figure 3).<sup>9,26</sup> At an ionic strength of 0.5  $\text{mol L}^{-1}$ , however, the uptake of the anions P and As decreased to about 80% while the uptake of the

cations Cd and Cu was still  $\sim 100\%$ . These results agree well with previous work.<sup>39</sup>

For the storage times tested, the recovery of analytes was in the acceptable range of  $\pm 10\%$  for the first 14 days with a slight increase in variation up to 47 days. After longer storage, the difference of the  $c_{\text{DGT}}$  values and the directly measured concentrations, as well as the standard deviation of the  $c_{\text{DGT}}$  concentrations, increased considerably (Figure 3). These results suggest that the HR-MBG should be used within 47 days after production to obtain an optimal DGT response for all tested analytes.

**Limit of Detection and Limit of Quantification.** Blank values, limits of detection, and limits of quantification for the measurements of digested gels and LA-ICPMS measurements are given in Table 1. The blank levels of P and Cd with 130 and

**Table 1. Blank and Background Equivalent Concentration (BEC), LOD, and LOQ for Gel Digests and LA-ICPMS Measurements<sup>a</sup>**

	liquid ICPMS (gel digests) (ng cm <sup>-2</sup> )			LA-ICPMS (dried gels) (ng cm <sup>-2</sup> )		
	blank	LOD	LOQ	BEC	LOD	LOQ
As	$0.06 \pm 0.01$	0.5	1.6	3	0.8	2.8
P	$130 \pm 32$	96	320	225	34	113
Cd	$70 \pm 20$	60	200	44	39	130
Cu	$0.8 \pm 0.6$	1.8	5.9	18	1.5	5.0

<sup>a</sup>The LOD was calculated as three times the standard deviation of the blank gels and the LOQ as 10 times the standard deviation of the blank, respectively.

70 ng cm<sup>-2</sup>, respectively, were higher than those of Cu and As. The investigation of all the chemicals used showed small, but stable, background concentrations of P ( $40 \pm 4 \mu\text{g g}^{-1}$ ) and Cd ( $3.1 \pm 0.7 \mu\text{g g}^{-1}$ ) in the ether-based urethane polymer material (Hydromed D4). This background can be considerably reduced (to 65 ng cm<sup>-2</sup> P and 20 ng cm<sup>-2</sup> Cd) by washing Hydromed in laboratory grade water (1:15, m/v) with 4 successive water changes on a shaker prior to gel production. The swelling of the Hydromed during washing has to be compensated by drying at 80 °C for 15 h with compensation of the net weight loss by adding laboratory water type 1. However, the blank levels were homogeneously distributed on the gel and stable between gels from different production batches; therefore, they are compensated for by blank correction. The BEC levels for the LA-ICPMS analysis are given in Table 1 and are in the same range as the blank levels as determined by digestion and measurement of blank HR-MBG gels.

**LA-ICPMS Calibration.** Two exemplary laser ablation calibrations for  $^{63}\text{Cu}$  and  $^{65}\text{Cu}$  are shown in Figure 4. All slopes and regression coefficients are given in Table S-1, Supporting Information. The calibration lines were computed for 6 calibration standards. The working range was estimated on the basis of preliminary experiments and expected concentrations of target analytes in the respective soil. The selected working range allowed for a linear calibration of LA-ICPMS measurements which is not necessarily the case for this type of measurement.<sup>9</sup> The error bars in both, the  $x$  and  $y$ , directions clearly show that a reliable calibration based on DGT gels requires several data points over the concentration range.

**Chemical Imaging of Anions and Cations in Soil and the Rhizosphere.** For DGT chemical imaging, the use of very thin diffusion layers (10  $\mu\text{m}$  in this study) is necessary to

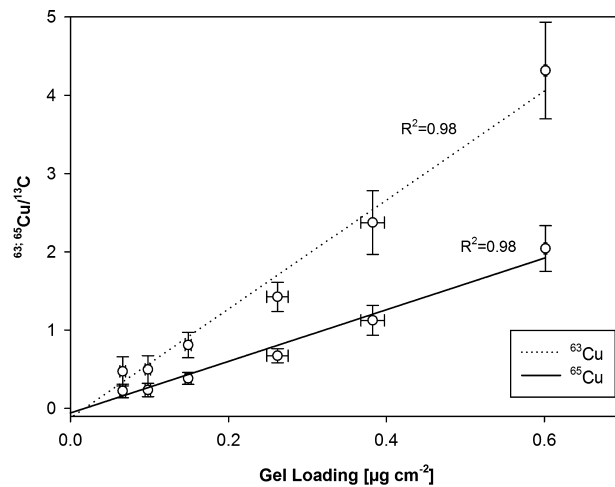


**Figure 4.** Exemplary calibration for  $^{63}\text{Cu}$  and  $^{65}\text{Cu}$  measured with LA-ICPMS. Error bars on the  $x$  axis represent the standard deviation of three replicates of digested standard gels. Error bars on the  $y$  axis represent the standard deviation of the measured  $\text{Cu}/^{13}\text{C}$  signal on the standard gel.

minimize lateral solute diffusion in the diffusion layer and thus image blurring. However, the solute mass accumulated on DGT samplers with thin diffusion layers will not increase proportionally compared to the standard diffusion layer thickness ( $\sim 940 \mu\text{m}$ ) if desorption from soil governs the solute supply to the DGT sampler. Lehto et al. showed this effect for DGT measurements of Cu and Cd on two soils, where the accumulated mass increased  $\sim 3$ -fold at most for a 80-fold in decrease in  $\Delta g^{28} c_{\text{DGT}}$  values calculated for thin diffusion layers will therefore often be unusually low compared to the standard  $\Delta g$ , which can cause confusion if DGT chemical images are reported as  $c_{\text{DGT}}$  values. Generally, the interpretation of DGT chemical images is often done based on the relative distribution of the analytes rather than on absolute concentrations. To avoid misinterpretation, the effect of decreased  $\Delta g$  should be pointed out when reporting DGT images as  $c_{\text{DGT}}$  values. Alternatively, images can be given as  $f_{\text{DGT}}$  values, which show the actual flux that may be increased for thin  $\Delta g$ , but which are not normalized for the diffusion layer thickness (cf. Equations 1 and 2).

Chemical images of the distribution of P, As, Co, Cu, Mn, and Zn in the rhizosphere of *Z. mays* L. are shown in Figure 5 as  $f_{\text{DGT}}$  values. A line scan raster of 69 laser lines (300  $\mu\text{m}$  line spacing) with 287 readings along each line was measured on the dried resin gel, resulting in a 19,803 pixel image for every measured isotope. This equals a spatial resolution of  $122 \times 300 \mu\text{m}$ . If required, the spatial resolution in LA-ICPMS analysis can be increased considerably. It is important to note, however, that the achievable spatial resolution is in most cases limited by the homogeneity of the resin distribution in the DGT gel and diffusive blurring during analyte uptake and not by the instrumental resolution limits of  $\sim 2 \mu\text{m}$ .<sup>40</sup> With these features, the HR-MBG is a novel gel with the unique capability of simultaneously sampling cationic and anionic solute species for high resolution chemical imaging in porous media. The more complicated gel preparation compared to other cation and anion binding gels and the need for microwave-assisted digestion render the HR-MBG a specialized gel for DGT imaging applications.

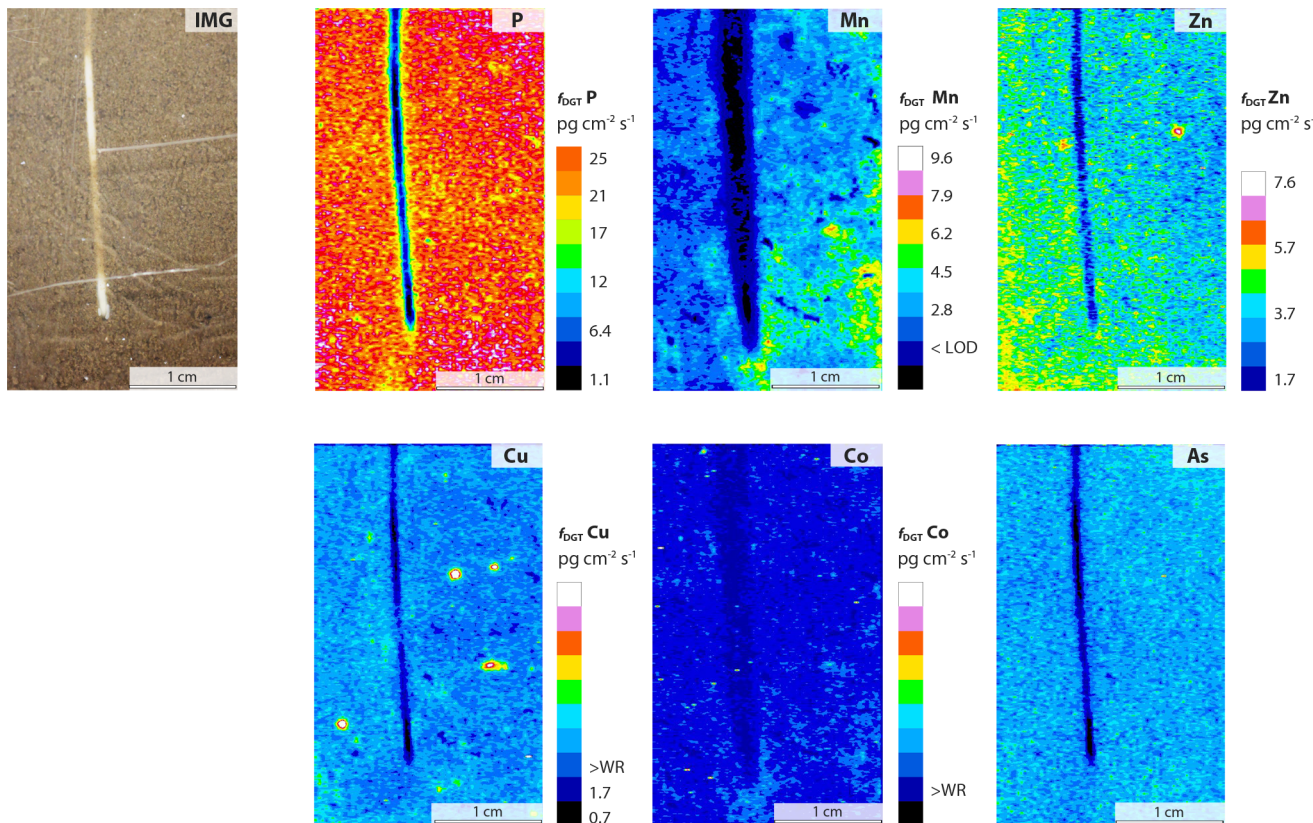


**Figure 5.** A photograph of a root grown in a rhizotron soil (IMG) is shown along with chemical images obtained by DGT–LA-ICPMS of P, Mn, Zn, Cu, Co, As, and Cd. The  $f_{\text{DGT}}$  concentrations were calculated on the basis of eq 2. The image for As is not calibrated here and thus shows the relative intensity of the As signal. LOD denotes the limit of detection; WR denotes the upper limit of the working range.

It can be seen that the analytical approach leads to 2D images providing sufficient resolution for further interpretation. As expected, phosphorus is depleted near the maize root in a very narrow area.<sup>13,41</sup> The depletion zone of Mn was larger, extending about 1 mm into the soil. DGT-labile Mn was strongly depleted in the center of this zone and showed a clear gradient into the surrounding bulk soil. Zinc was depleted in a very narrow area just along the root. Interestingly, we observed concentration hotspots of Cu and Zn, most of them not located in direct vicinity of the root. Although we can only speculate about their origin, hotspots of microbial activity and their complex interactions mobilizing these metals during, e.g., the decomposition of organic matter seem to be a likely explanation for this observation, similar to trace metal mobilization in sediments.<sup>16,17,42</sup> The loading of Co on the DGT gel was below the working range for large parts of the image. Nevertheless, we were able to observe Co depletion in a zone of about 1 mm around the root. The mapping of As was initially not considered for calibration due to the very low concentrations expected in this soil. However, the images of Co and As still reveal that even at very low count rates close to the LOD a depletion zone can be distinguished from the bulk soil and chemical imaging can visualize the removal of elements in the rhizosphere even at very low concentration.

## CONCLUSIONS

We developed a novel DGT resin gel, the HR-MBG, which facilitates the simultaneous high-resolution LA-ICPMS imaging of anionic and cationic solutes. It is the first DGT gel employing an ether-based urethane polymer hydrogel (Hy-

dromed D4). Thin layers ( $100 \mu\text{m}$ ) of this gel are highly tear-proof and geometrically stable, rendering Hydromed D4 superior to thin polyacrylamide gel layers. This material may also serve as matrix for other thin-layer DGT gels. We report on performance tests of the novel HR-MBG for the anions As and P and the cations Cd and Cu, but the resins used (SPRIDA, Zr-hydroxide) make the gel suitable for a large variety of ion species. The gel can be used in similar environmental conditions as existing DGT gels (pH 4–8, ionic strength of 1–100 mmol L<sup>-1</sup>). The shelf life of the HR-MBG is 47 days, and the capacity is sufficiently high for deployment in uncontaminated natural environments with a normal range of solute concentrations of the target ions. With these features, the new HR-MBG is well suited for the accurate, simultaneous analysis of cation and anion distribution at high spatial resolution by LA-ICPMS.

## ASSOCIATED CONTENT

### Supporting Information

Setup and procedure of the chemical imaging experiment, hydration characteristics of the HR-MBG, slope and regression coefficients for the DGT LA-ICPMS calibration, and additional data for gel characterization of Co and Zn. This material is available free of charge via the Internet at <http://pubs.acs.org>.

## AUTHOR INFORMATION

### Corresponding Author

\*E-mail: jakob.santner@boku.ac.at.

### Notes

The authors declare no competing financial interest.

## ACKNOWLEDGMENTS

We acknowledge the funding of the project “Chemical imaging of phosphorus dynamics in the rhizosphere” (P23798-B16) by the Austrian Science Fund (FWF). We thank Vanessa Álvarez López (Instituto de Investigaciónes, Agrobiológicas de Galicia, Santiago de Compostela) for her generous help with the plant growth experiment.

## REFERENCES

- (1) Chapman, E. E. V.; Dave, G.; Murimboh, J. D. *Water, Air, Soil Pollut.* **2012**, *223*, 2907–2922.
- (2) Mason, S.; McLaughlin, M.; Johnston, C.; McNeill, A. *Plant Soil* **2013**, *1*–12.
- (3) Degryse, F.; Smolders, E.; Parker, D. R. *Eur. J. Soil Sci.* **2009**, *60*, 590–612.
- (4) Six, L.; Pypers, P.; Degryse, F.; Smolders, E.; Merckx, R. *Plant Soil* **2012**, *359*, 267–279.
- (5) Mason, S.; McNeill, A.; McLaughlin, M.; Zhang, H. *Plant Soil* **2010**, *337*, 243–258.
- (6) Zhang, H.; Davison, W.; Gadi, R.; Kobayashi, T. *Anal. Chim. Acta* **1998**, *370*, 29–38.
- (7) Zhang, H.; Davison, W. *Anal. Chem.* **1995**, *67*, 3391–3400.
- (8) Stockdale, A.; Davison, W.; Zhang, H. *Environ. Chem.* **2008**, *5*, 143–149.
- (9) Santner, J.; Prohaska, T.; Luo, J.; Zhang, H. *Anal. Chem.* **2010**, *82*, 7668–7674.
- (10) Zhang, H.; Zhao, F. J.; Sun, B.; Davison, W.; McGrath, S. P. *Environ. Sci. Technol.* **2001**, *35*, 2602–2607.
- (11) Davison, W.; Fones, G. R.; Grime, G. W. *Nature* **1997**, *387*, 885–888.
- (12) Six, L.; Smolders, E.; Merckx, R. *Plant Soil* **2013**, *366*, 49–66.
- (13) Santner, J.; Zhang, H.; Leitner, D.; Schnepf, A.; Prohaska, T.; Puschenreiter, M.; Wenzel, W. W. *Environ. Exp. Bot.* **2012**, *77*, 219–226.
- (14) Ding, S.; Jia, F.; Xu, D.; Sun, Q.; Zhang, L.; Fan, C.; Zhang, C. *Environ. Sci. Technol.* **2011**, *45*, 9680–9686.
- (15) Shuttleworth, S. M.; Davison, W.; Hamilton-Taylor, J. *Environ. Sci. Technol.* **1999**, *33*, 4169–4175.
- (16) Devries, C. R.; Wang, F. *Environ. Sci. Technol.* **2003**, *37*, 792–797.
- (17) Teasdale, P. R.; Hayward, S.; Davison, W. *Anal. Chem.* **1999**, *71*, 2186–2191.
- (18) Warnken, K. W.; Zhang, H.; Davison, W. *Anal. Chem.* **2004**, *76*, 6077–6084.
- (19) Motelica-Heino, M.; Naylor, C.; Zhang, H.; Davison, W. *Environ. Sci. Technol.* **2003**, *37*, 4374–4381.
- (20) Gao, Y.; Lehto, N. *Talanta* **2012**, *92*, 78–83.
- (21) Zhang, Y.; Mason, S.; McNeill, A.; McLaughlin, M. J. *Talanta* **2013**, *113*, 123–129.
- (22) Mason, S.; Hamon, R.; Nolan, A.; Zhang, H.; Davison, W. *Anal. Chem.* **2005**, *77*, 6339–6346.
- (23) Colmer, T. D. *Plant, Cell Environ.* **2003**, *26*, 17–36.
- (24) Hansel, C. M.; Fendorf, S.; Sutton, S.; Newville, M. *Environ. Sci. Technol.* **2001**, *35*, 3863–3868.
- (25) Davison, W.; Zhang, H. *Nature* **1994**, *367*, 546–548.
- (26) Ding, S.; Xu, D.; Sun, Q.; Yin, H.; Zhang, C. *Environ. Sci. Technol.* **2010**, *44*, 8169–8174.
- (27) Odian, G. *Principles of polymerisation*; John Wiley and Sons, Inc.: Hoboken, NJ, 2004.
- (28) Lehto, N. J.; Davison, W.; Zhang, H. *Environ. Chem.* **2012**, *9*, 415–423.
- (29) BIO-RAD. BIO-RAD Laboratories. [http://www3.bio-rad.com/webmaster/pdfs/9184\\_Chelex.PDF](http://www3.bio-rad.com/webmaster/pdfs/9184_Chelex.PDF) (14.11.2013), 1998.
- (30) IUPAC. McNaught, A. D., Wilkinson, A., Eds.; *Compendium of Chemical Terminology*; Blackwell Scientific Publications: Oxford, 1997.
- (31) *World Reference Base for Soil Resources 2006, first update 2007*; World Soil Resources Reports; FAO: Rome, 2007.
- (32) Stahl, H.; Warnken, K. W.; Sochaczewski, L.; Glud, R. N.; Davison, W.; Zhang, H. *Limnol. Oceanogr.: Methods* **2012**, *10*, 389–401.
- (33) Zhang, H.; Davison, W. *Anal. Chim. Acta* **1999**, *398*, 329–340.
- (34) Garmo, Ø. A.; Røyset, O.; Steinnes, E.; Flaten, T. P. *Anal. Chem.* **2003**, *75*, 3573–3580.
- (35) Fitz, W. J.; Wenzel, W. W.; Zhang, H.; Nurmi, J.; Štipek, K.; Fischerová, Z.; Schweiger, P.; Köllensperger, G.; Ma, L. Q.; Stingeder, G. *Environ. Sci. Technol.* **2003**, *37*, 5008–5014.
- (36) Huynh, T.; Zhang, H.; Noller, B. *Anal. Chem.* **2012**, *84*, 9988–9995.
- (37) Schachtschabel, P.; Blume, H. P.; Scheffer, F. *Lehrbuch der Bodenkunde*; Spektrum Akademischer Verlag: Heidelberg, 2002; p 145.
- (38) Bortun, A.; Bortun, M.; Pardini, J.; Khainakov, S. A.; Garcia, J. R. *Mater. Res. Bull.* **2010**, *45*, 1628–1634.
- (39) Peters, A. J.; Zhang, H.; Davison, W. *Anal. Chim. Acta* **2003**, *478*, 237–244.
- (40) Harper, M. P.; Davison, W.; Tych, W. *Aquat. Geochem.* **1999**, *5*, 337–355. Sochaczewski, L.; Davison, W.; Zhang, H.; Tych, W. *Environ. Chem.* **2009**, *6*, 477–485.
- (41) Bhat, K. K. S.; Nye, P. H. *Plant Soil* **1973**, *38*, 161–175.
- (42) Wenzel, W. W. *Plant Soil* **2009**, *321*, 385–408.